The Effect of Residual Stresses on Fatigue of Butt Joints

A theoretical model simulating the effect of residual stresses in welded butt joints agrees well with the available experimental data

BY T. N. NGUYEN AND M. A. WAHAB

ABSTRACT. In this paper, a theoretical analysis of the effect of residual stresses on the fatigue behavior of welded butt joints was developed by using linear elastic fracture mechanics (LEFM), superposition principle and finite element approaches. Various configurations of residual stresses in welded butt joints were considered and corresponding residual stress intensity factors were calculated by using Bueckner's and Kanazawa's weight functions for an edge and a central through-thickness crack in finite plate, respectively. Newman-Raju's empirical equation was also used for surface cracks. Fatigue life of butt joint welds subjected to various stress-induced treatments was calculated by using Paris's law with the effective range of stress intensity factor for zero-to-tensile loading (R = 0) and compared with the available experimental data.

Compressive residual stresses introduced on the surface of the welded joints by various surface treatments, such as single- and multiple-point hammer peening, steel shot peening, glass peening, stress peening (loaded and peened) and tensile preloading, improved fatigue life and fatigue strength of welded butt joints. The improvement of fatigue life is due to the early state of crack propagation with the size of crack length not exceeding the depth of the compressive residual stress field.

It was also found that the effect of a low level of compressive residual stress (less than 62 MPa) in terms of the fatigue strength improvement is of the same order as the effect of a postweld thermal stress relieving process. The contribution of hardness of the treated material to the improvement of fatigue life is obvious at a high level of compressive residual stresses.

T. N. NGUYEN is a Ph.D. student and M. A. WAHAB is a Senior Lecturer in the Dept. of Mechanical Engineering, The University of Adelaide, Australia.

Introduction

Fatigue behavior of welded stuctures is complicated by many factors intrinsic to the nature of welded joints. Normally, crack-like discontinuities such as slag inclusions, gas pores, incomplete fusion at the weld root or undercut at weld toes may be introduced into welded joints. Residual stresses that arise in welded joints as a consequence of incompatible thermal strains caused by heating and cooling cycles during the welding process also affect the fatigue behavior of the welded structures. Especially, a tensile residual stress of the order of yield magnitude may exist in as-welded structures, and may cause a detrimental effect on the fatigue behavior of the welded structure (Ref.1).

KEY WORDS

Residual Stress
Fatigue Life
Fatigue Strength
Welded Butt Joint
Surface Crack
Edge Crack
Central Crack
Stress Intensity Factor
Shot Peening

Many studies related to the effect of residual stress in welded structures have shown that fatigue strength of welded structures may be improved by reducing the effect of tensile residual stress in as-welded components (Refs. 2–4) or even by mechanical treatments so that the compressive residual stresses are induced in welded joint regions (Refs. 5–7). This may be conducted by postweld thermal relieving heat treatments or mechanical peening processes. However, in practice, the majority of welded steel structures are not suitable for heat treatments and are put into service before welding residual stresses could be relieved. It means that surface treatments are the most convenient measures for the welded structures to improve their fatigue performance in terms of eliminating the effect of postwelding residual stresses.

It is well known that regions of compressive residual stresses retard the rate of fatigue crack growth while tensile residual stresses produce the opposite effect (Ref. 8). The effect of surface treatments in terms of introducing compressive residual stresses to improve fatigue strength of welded joints are reported by many authors (Refs. 5–7, 9). However, the theoretical analysis of the effect of compressive residual stress in welded structures on the improvement of fatigue strength and fatigue life is still not clear. Therefore, this study aims to reveal the theoretical explanations for the fatigue strength improvement due to the compressive residual stress introduced by various postweld surface treatments.

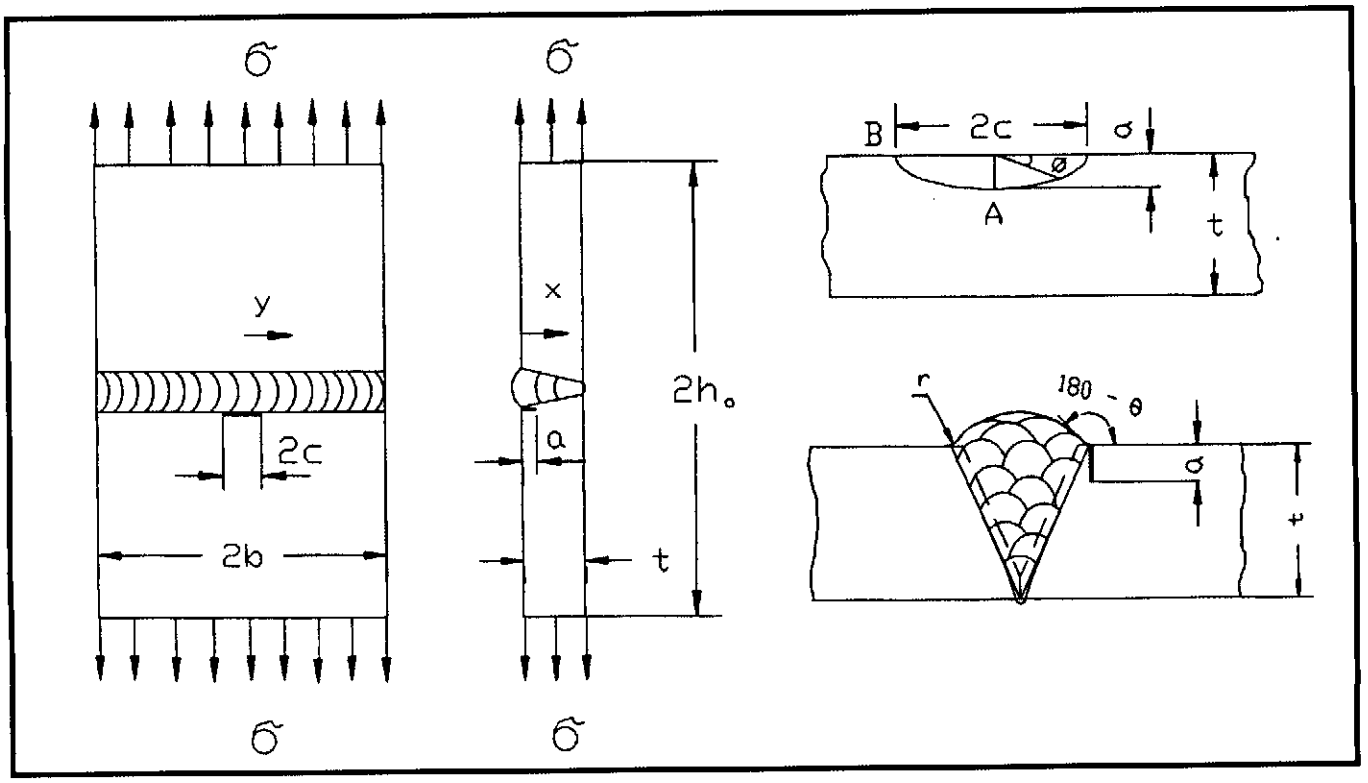

Fig. 1 — Surface crack model for transverse welded butt joint (Mode 1).

In this study, residual stress distributions are not measured but assumed, and based on the number of studies, related to residual stresses in as-welded and shot-peened welded joints (Refs. 2–9). A model for semi-elliptical surface cracks originating at the weld toe region in the center of the welded plate was constructed to evaluate the contribution of the weld geometry and residual stresses to the stress intensity factor based on linear elastic fracture mechanics (LEFM), superposition principle and finite element approaches. As a result, the effect of residual stresses on the fatigue behavior of welded joints can also be evaluated.

Modeling Concepts

When a fatigue crack is propagating through a residual stress field in a welded plate, the stress intensity at the crack front is influenced by the combined effect of local residual stress and the stress resulting from externally applied stress. The latter is influenced by weld geometry and crack-like inclusions in the weld. It means that the effective stress intensity factor of the crack front is obtained by superimposing the solutions for the stress intensity factor due to residual stresses and the solutions for the stress intensity factor due to external loading (Ref. 10) as follows:

$$K_{eff} = K_{app} + K_{res} \quad (1)$$

Then the rate of fatigue crack growth can be described in Paris's equation in terms of the range of effective stress intensity factors as:

$$da/dN_p = C\cdot(\Delta K_{eff})^m \quad (2)$$

It is ohvious from Equations 1 and 2 that the fatigue life and fatigue strength of the welded joint subjected to a residual stress field can be evaluated if the solutions for the stress intensity factors K_{res} and K_{app} are known. Solutions for the stress intensity factor due to various crack geometries are available from the literature in fracture mechanics and can be used for the fatigue assessment of welded structures. In this study, a semi-elliptical surface crack with aspect ratio a/c = 0.2 (Fig. 1) is assumed to be located at the weld toe as a result of weld toe undercut of the order of 0.1 mm (a_i = 0.1 mm). This conservative assumption was also supported by other researchers (Refs. 11, 12). Then the total fatigue life of the welded plate can be considered as the number of cycles needed for this initiated semi-elliptical surface crack to propagate through the thickness of the welded plate.

An empirical solution for the stress intensity factor due to a semi-elliptical surface crack in the center of a finite plate in Mode I loading is given by Newman and Raju (Ref. 13) as follows:

$$K_{sc} = S\cdot\sqrt{(\pi a/Q)}\cdot F(a/t,\ a/c,\ c/b,\ \phi) \quad (3)$$

However, by using this solution, the effect of residual stresses and weld geometry on the welded joint cannot be included because it only considers a flat plate with a surface crack subjected to remotely applied constant axial stress. No local stress raisers or residual stress conditions have been considered in this solution. In order to overcome this ohstacle, the weight function method was applied to calculate the stress intensity factor, and it is necessary to assume the "similarity effect" between the stress intensity values of notched and unnotched bodies due to various crack shapes. It means that the ratios of stress intensity values between the notched and unnotched body are the same for surface crack, edge crack or central through-thickness crack. This assumption is already supported by other researchers (Refs. 14, 15).

When a welded joint is considered as a notched body, the following equations can be written:

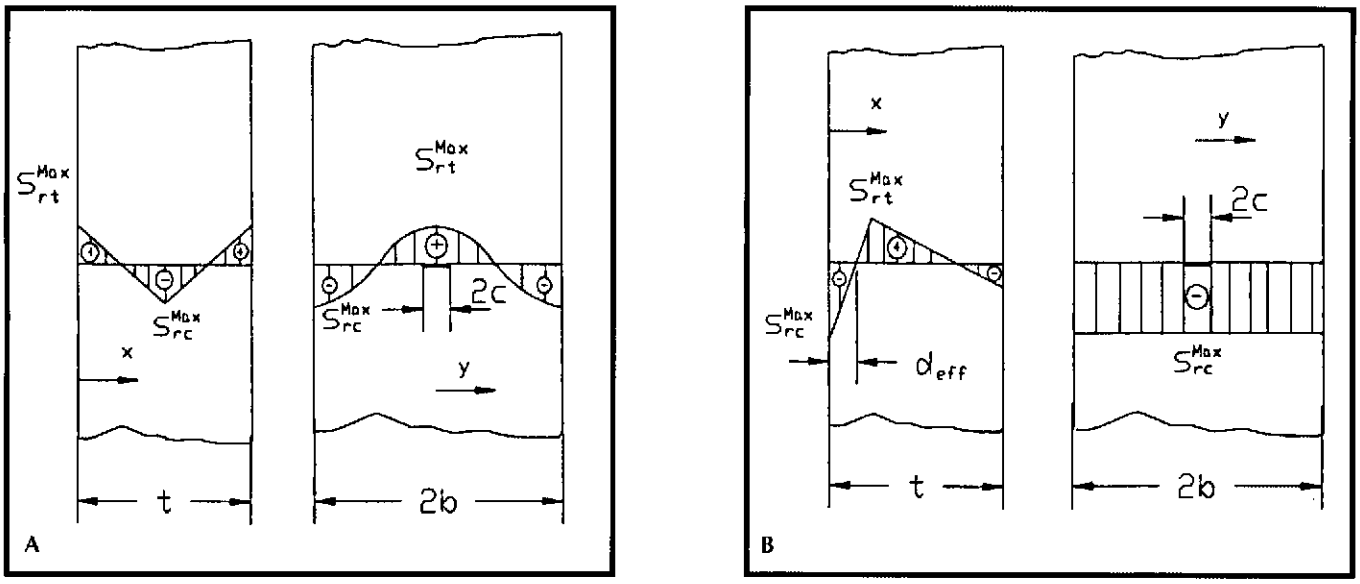

Fig. 2 — Patterns of residual stress fields through thickness and along the width of welded plate.

$$K^{W}_{sc,A}/K_{sc,A} = k^{W}_{eff}/K_{eff} = M^{A}_{k,r} \quad (4)$$

$$K^{W}_{sc,B}/K_{sc,B} = K^{W}_{cen}/K_{cen} = M^{B}_{k,r} \quad (5)$$

Using Equations 4 and 5, the stress intensity factors due to the semi-elliptical surface crack at the weld toe for point A at a certain depth and surface crack front point B (Fig. 1) can be calculated if the stress intensity solutions for an edge crack and a central through-thickness crack on a welded and flat plate are known.

Using Bueckner's weight functions for an edge crack in a finite plate (Ref. 16) and Kanazawa's weight function for a central through-thickness crack (Ref. 8), stress intensity factors can be calculated as follows:

$$K^{edl} = 2\cdot\int_0^a S(x)\cdot m(a,x)\cdot dx \quad (6)$$

$$K_{cen} = 2\cdot\int_0^c S(y)\cdot G(c,y)\cdot dy \quad (7)$$

When S(x) and S(y) are the local stress distributions along potential crack directions x and y, respectively (Fig. 1), then each of them should be a resulting stress due to the residual stresses and local stress subjected to external loading in the proper direction.

By using two-dimensional finite elements, the local stress distributions subjected to weld geometry can be calculated and fitted into the polynomial form for later use in the calculation of the stress intensity factor. The residual stress distribution patterns along x and y directions of the transverse-welded butt joints are assumed and based on the studies related to residual stresses from the literature (Refs. 2–10). The equations used for modeling of residual stresses in the as-welded condition and surface-treated conditions are given in the Appendix.

In this study, a transverse-welded butt joint with moderate weld geometry has been chosen with r = 1 mm, Θ = 30 deg, t = 6.35 mm (Fig. 1) with the assumption that geometry of the butt welded joint is unchanged along the plate width. Residual stresses in the as-welded condition and surface-treated condition along x and y directions are assumed to follow the patterns shown in Fig. 2. With the above assumptions, the stress intensity magnification factors $M^{A}_{k,r}$ and $M^{B}_{k,r}$ due to the combined effect of weld geometry and residual stresses can be obtained. ΔK^{A}_{eff} and ΔK^{B}_{eff} can also be obtained. The crack-growth rates were calculated by assuming that Equation 2 is obeyed independently at points A and B at the crack front, and therefore, Equation 2 can be rewritten as:

$$da/dN_p = C_A\cdot(\Delta K^{A}_{eff})^m \quad (8)$$

$$dc/dN_p = C_B\cdot(\Delta K^{B}_{eff})^m \quad (9)$$

where $C_B = 0.9^m\ C_A$ as suggested by Newman and Raju (Ref. 13).

By integrating Equations 8 and 9 simultaneously, the fatigue life and fatigue strength of a welded butt joint subjected to various levels of residual stresses in the as-welded condition and in the surface-treated conditions can be evaluated. A computer program was written to facilitate the numerical procedures discussed above and Simpson's rule was used for the calculation of integrals. The material constants of Paris's equations was assumed as m = 3, $C_A = 3 \times 10^{-13}$ mm/cycle as recommended by Maddox (Ref. 1) for a wide range of structural steels. The failure criteria were chosen for the instant when the depth of the semi-elliptical surface crack in the through-thickness direction reached half of the plate thickness (a_f = 0.5t) or the effective range of stress intensity factor exceeded the fracture toughness of the base metal (whichever occurs first).

Results and Discussion

In this study, various levels of compressive residual stress fields introduced by particular postweld surface treatments such as single- or multiple-hammer peening (S_r = – 152 and – 172 MPa), glass or steel shot peening (S_r = – 62 and –110 MPa) and stress peening (loaded and peened) (S_r = –172 MPa) were assumed based on available experimental data (Ref. 5). Maximum tensile residual stress in the as-welded condition was assumed to be at the level of the yield stress (S_r = 300 MPa), and low levels of tensile residual stresses are also assumed to simulate the stress-relieved condition (S_r = 0 and S_r = 14 MPa). Respective residual stress patterns are shown in Fig. 2. For the case of compressive residual stresses introduced by surface treatments, the peak of the tensile residual stresses along the through-thickness direction (x-direction) are assumed to be half of the order of magnitude of induced compressive residual stresses at the treated surfaces.

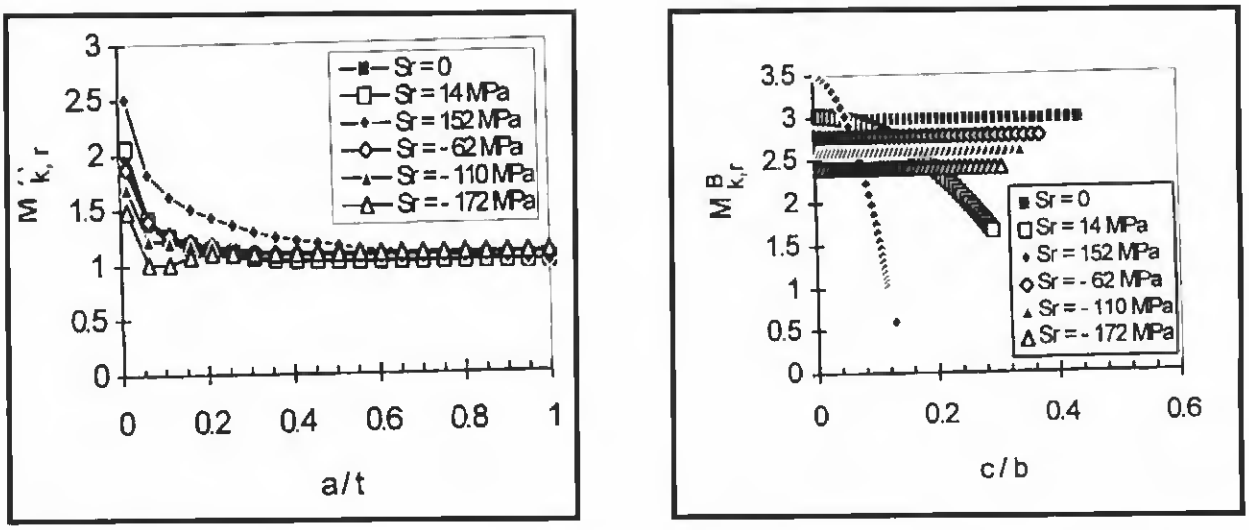

Fig. 3 — Effect of residual stresses on stress intensity magnification factor. A — Effect of residual stress on $M^A_{k,r}$; B — effect of residual stress on $M^B_{k,r}$.

This assumption was based on the experimental results carried out by Wahab (Ref. 5). Using the effective depth of surface treatment d_{eff} taken from experimental data (Ref. 5) and the above assumption, the peak of self-balanced compressive residual stress at the opposite side of the treated surface can be evaluated as follows:

$$S^{*}_{rc} = S_r \cdot (t - 3 \cdot d_{eff}) / (2 \cdot t - 3 \cdot d_{eff}) \qquad (10)$$

The value of d_{eff} was 0.2 and 0.43 mm for glass and steel shot peening, 0.76 and 0.69 mm for single-point and multiple-point hammer peening, and 0.7 mm for stress peening, respectively (Ref. 5).

For the as-welded condition, the magnitude of peak compressive residual stress is assumed to be the same as the maximum tensile residual stress at the weld toe surface and is located at the middle of the plate thickness ($S^{max}_{rc} = -S_r$). The distribution of surface residual stresses along the plate width (y-direction) was assumed constant for each case of surface treatments and was assumed to follow a cosine pattern in the case of the as-welded condition with the peak tensile residual stress located in the middle of the welded plate — Fig. 2.

Figure 3 shows the variation of magnification factors $M^A_{k,r}$ and $M^B_{k,r}$ due to the combined effect of weld geometry and residual stresses calculated for assumed butt weld geometry (r = 1 mm, Θ = 30 deg, t = 6.35 mm). Figure 3A shows that compressive residual stresses reduce the value of $M^A_{k,r}$ at an early stage of crack growth, while tensile residual stresses tend to increase it. However, the effect of the low level of compressive residual stress on the order of 62 MPa is coincidental with the effect of a stress-relieved condition ($S_r = 0$ and $S_r = 14$ MPa).

Figure 3B shows the effect of residual stresses on the $M^B_{k,r}$ value across the width of the welded plate. The values of $M^B_{k,r}$ for each surface treatment are constant as a result of the same level of compressive residual stress introduced at the plate surface. However, values of $M^B_{k,r}$ were reduced compared with a "perfect" stressed-relieved condition ($S_r = 0$) subjected to a particular level of compressive residual stresses. In the as-welded condition due to the presence of tensile residual stresses, the values of $M^B_{k,r}$ are increased in an early stage of crack growth compared with the "perfect" stressed-relieved condition ($S_r = 0$) but decreased after the crack reached the length of the order of 0.08 times the plate width (c/b = 0.08). This effect of tensile residual stresses depends on the magnitude of peak tensile residual stresses —

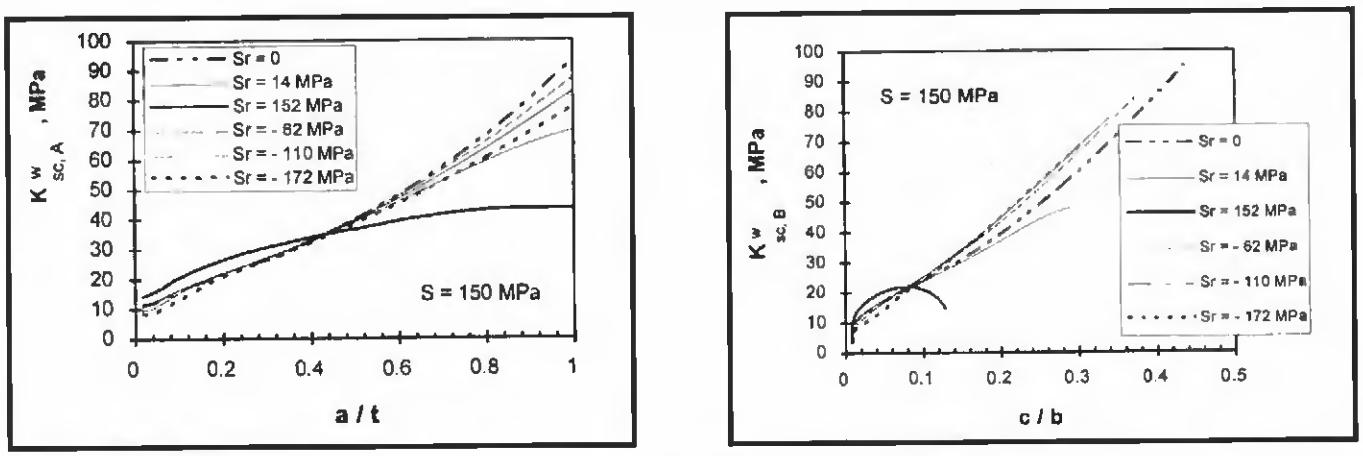

Fig. 4 — Effect of residual stresses on stress intensity factors. A — Effect of residual stress on $K^W_{sc,A}$; B — effect of residual stress on $K^W_{sc,B}$.

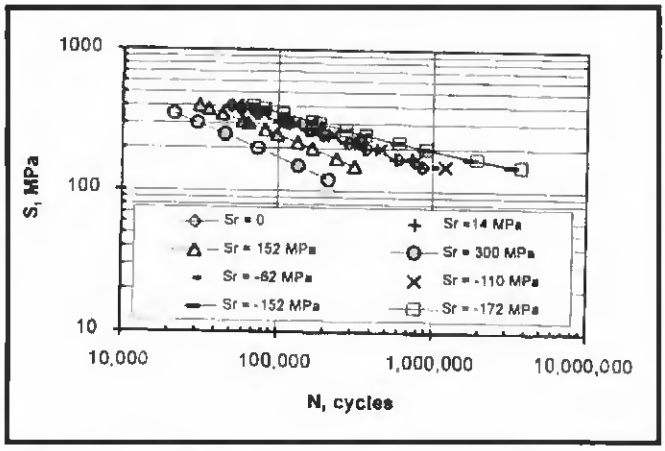

Fig. 5 — Effect of residual stresses in welded butt joints on S-N curve.

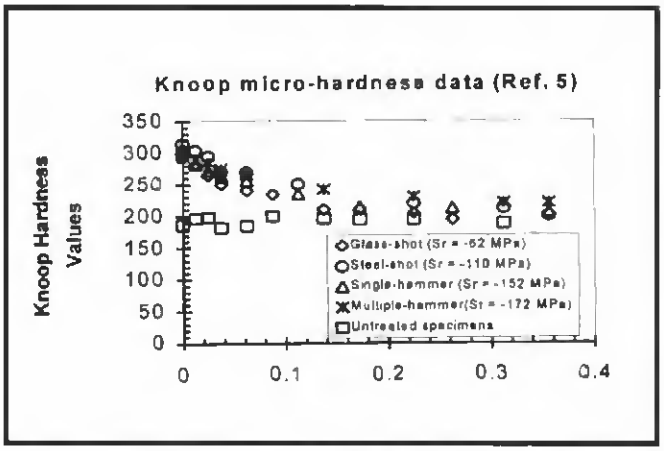

Fig. 6 — Knoop microhardness of treated and untreated surfaces vs. depth of work hardening (Ref. 5).

Fig. 3B.

Figure 4 shows the values of the stress intensity factors $K^W_{sc,A}$ and $K^W_{sc,B}$ for the case of applied stress S = 150 MPa. Figure 4A shows that the stress intensity factor $K^W_{sc,A}$ is increased by tensile residual stress and decreased by compressive residual stress due to the early stage of crack growth compared with that in a stress-relieved condition. As a result, compressive residual stress improves the fatigue life of a welded butt joint, while tensile residual stress decreases it. This conclusion is consistent with the results reported by other authors (Refs. 2–9). However, after the crack reached the length of the order of 0.45 times plate thickness (0.45t), the stress intensity value $K^W_{sc,A}$ begins to decrease by the effect of tensile residual stress in the as-welded condition, while compressive residual stresses continue to decrease the value of $K^W_{sc,A}$ compared with the stress-relieved state. It means that fatigue crack growth at an early stage (crack length less than 0.45 times plate thickness) dominates the whole fatigue life.

Figure 4A also shows that there is no significant difference between the effect of low-tensile residual stress simulating a stress-relieved state (S_r = 0 and S_r = 14 MPa) and at a low level of compressive stress on the order of 62 MPa. It means that the effect of low-compressive residual stress (less than 62 MPa) and the effect of the stress-relieving process on the fatigue behavior of welded butt joints are almost the same.

Figure 4B shows the effect of residual stresses on the stress intensity factor $K^W_{sc,B}$ in the way similar to its effect on $K^W_{sc,B}$. However, after the transition point at the crack length on the order of 0.08 times plate width (0.08b), the effect of residual stress on $K^W_{sc,B}$ has a new feature. The values of $K^W_{sc,B}$ begin to increase by compressive residual stresses introduced by surface treatments. This can be explained by the change of residual stress patterns in a later stage of crack propagation.

Figure 5 shows the S-N fatigue curves in terms of the effect of residual stresses in welded butt joints. It is obvious that fatigue strength was improved by compressive residual stresses, while it was reduced by tensile residual stresses. The effect of the stress-relieved process and low compressive residual stresses (less than 62 MPa) are in the same scatter range.

Figure 6 shows a comparison between Knoop microhardness of the treated surfaces and untreated surface measured through the depth of work hardening (Ref. 5). It is obvious from this figure that the microhardness values of the treated surfaces corresponding to various shot peenings are much higher compared with that of the untreated surface. This behavior of treated surfaces becomes less significant as the depth of work hardening increases further.

Figure 7 shows the comparison between calculated data of fatigue life with the available data (Ref. 5). It shows that the ratios between the experimental and predicted fatigue life are from 0.5 to 2.5. This difference between calculated life and experimental data is reasonable as the standard deviation (SD) of the log of experimental fatigue life data, log(N), is of the order of 0.201 (Ref. 5), *i.e.*, 95% confidence limits of fatigue life (mean(N) ±2SD) (Ref. 1) are 0.4N and 2.52N. This indicates that the prediction by the model developed in this study is acceptable as it gives the prediction with the same error as the typical scatter band of fatigue life that occurs in fatigue testing practices.

Furthermore, Fig. 7 also shows that the difference between the experimental and predicted fatigue life tends to increase as the values of induced compressive residual stresses increase. It suggests that high microhardness of treated surfaces (Fig. 6) must have an accompanying effect beneficial for the fatigue life of welded butt joints. This conclusion is consistent with the effect of hardness on the improvement of fatigue life reported by Heeschen

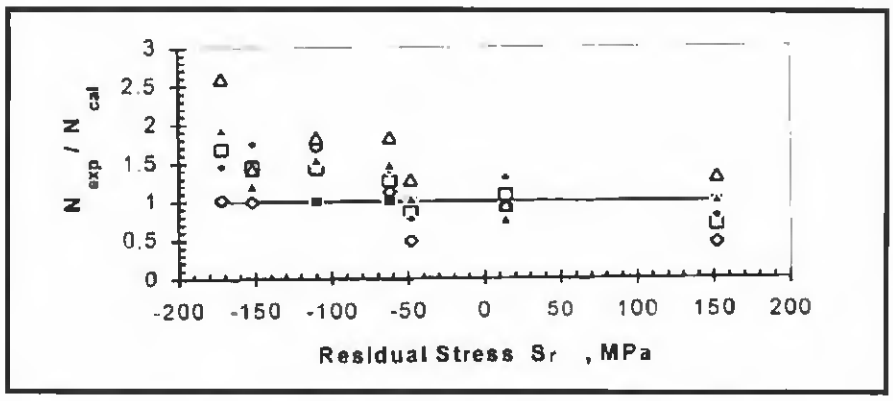

Fig. 7 — Comparison of calculated fatigue life data with the available data (Ref. 5).

and Wohlfahrt (Ref. 6).

Conclusions

From the theoretical analysis of the effect of residual stresses in welded hutt joints on its fatigue behavior, the following important condusions can be drawn:

1) Compressive residual stresses induced on the surface of welded joints by various surface treatment methods, such as single- or multiple-point hammer peening, steel or glass shot peening, stress peening (loaded and peened) or tensile preloading, improve fatigue life and fatigue strength of welded joints.

2) The improvement of fatigue life is due to the early stage of crack propagation with the size of crack length not exceeding the depth of compressive residual stress field. After that length, the induced compressive residual stresses have a nonsignificant effect on fatigue life.

3) A low level of compressive residual stresses (less than 62 MPa) induced by surface treatment in terms of fatigue strength improvement is of the same order as the improvement obtained by postweld thermal stress relieving treatment.

4) The contribution of surface hardness of the treated material on the improvement of fatigue strength is obvious at high levels of induced compressive residual stresses.

This analysis shows a basic understanding of the effect of residual stresses on fatigue crack propagation life and gives a good explanation for postweld surface treatments commonly used in practice to improve fatigue performance of welded structures. It also gives suggestions for more efficient use of postweld surface treatments for particular cases in engineering practice.

References

1. Maddox, S. J. 1991. *Fatigue Strength of Welded Structures*. Cambridge University Press, London, England.

2. Mateffy, V. K., Mikan, J. M., and Abel, A. 1984. Fatigue of welded joints — the effect of stress relieving. *Proceeding of Ninth Australasian Conference on Mechanics of Structures and Materials*, ASCMS 9, Published by the University of Sydney, Sydney, Australia.

3. Miki, C., and Mori, T., *et al.* 1986. Effect of stress ratio and tensile residual stress on near threshold fatigue crack growth. *Structural Eng. and Earthquake Eng.* 3(1): 175–182.

4. Wohlfahrt, H., and Heeschen, J. 1986–89. Possibilities for the improvement of the fatigue strength of butt welded joints of high strength structural steels. *Proceedings of IMechE* Vol. II.

5. Wahab, M. A. 1984. Fatigue life estimation of welded structures, unpublished Ph.D. thesis, The University of Alberta, Edmonton, Canada.

6. Heeschen, J., and Wohlfahrt, H. 1986. Assessment of the influence of shot peening on the fatigue strength of butt welded joints. *Residual Stresses in Science and Technology*, Vol. 2, Symposium of International Conference on Residual Stresses, Germany, pp. 467–476.

7. Desvignes, M., *et al.* 1986. Fatigue processing of shot peened steel. *Residual Stresses in Science and Technology*, Vol. 2, Symposium of International Conference on Residual Stresses, Germany, pp. 441–448.

8. Nelson, D. V. 1982. Effect of residual stress on fatigue crack propagation, *Residual Stress Effects in Fatigue*. ASTM STP 776, pp. 172–194.

9. Kim, Chongmin, and Diesburg, O. E., *et al.* 1982. Effect of resirlual stress on fatigue fracture of case-hardened steels — An analytical model. *Residual Stress Effects in Fatigue*. ASTM STP 776, pp. 224–234.

10. Elber, W. 1974. Effect of shot peening residual stresses on the fracture and crack growth properties of D6AC steel. *Fracture Toughness and Slow-Stable Cracking*. ASTM STP 569, American Society for Testing and Materials, pp. 45–58.

11. Lawrence, Jr., F. V. 1973. Estimation of fatigue crack propagation life in butt welds. *Welding Journal* 52: 213–220.

12. Maddox, S. J. 1970. Calculating the fatigue strength of welded joints using fracture mechanics. *Metal Construction and British Welding Journal*, pp. 327–331.

13. Newman, Jr., J. C., and Raju, I. S. 1981. An empirical stress-intensity factor equation for the surface crack. *Engineering Fracture Mechanics* 15(1–2): 185–192.

14. Niu, X., and Glinka, G. 1989. Stress intensity factors for semi-elliptical surface cracks in welded joints. *Inter. Journal of Fracture*, Vol. 40, pp. 255–270.

15. Foth, J., *et al.* 1986. Short crack phenomena in high-strength aluminium alloy and some analytical tools for their prediction. *The Behavior of Short Fatigue Cracks*, EGF Pub. 1, Mechanical Engineering Publications, London, England, pp.353–368.

16. Parker, A. B. 1981. *The Mechanics of Fracture and Fatigue* (An Introduction), London - New York E. & F.N. Spon Ltd.

Nomenclature

r	weld toe radius of butt joint
Θ	weld bead flank angle
t	plate thickness
a	crack length (edge crack) also half-length of minor elliptical surface crack
b	half-width of cracked plate
c	half-length of major elliptical surface crack; also half-length of central through-thickness crack
h	half-length of cracked plate
ϕ	parametric angle of the ellipse
d_{eff}	effective depth of surface treatments
a_i	crack initiation length
a_f	final crack length
N_p	fatigue crack propagation life
N	number of fatigue cycles to failure
N_{cal}	number of fatigue cycles calculated by the model
N_{exp}	number of fatigue cycles from experimental data
C, m	material constants in Paris's equation
C_A, C_B	material constants in Paris's equation at points A and B of crack front, respectively
K_{app}	applied stress intensity factor
K_{res}	residual stress intensity factor
k_{eff}	effective stress intensity factor
ΔK_{eff}	range of effective stress intensity factor
ΔK^A_{eff}	range of effective stress intensity factor at A
ΔK^B_{eff}	range of effective stress intensity factor at B
K_{ed}	stress intensity factor for edge crack in finite plate
K_{cen}	stress intensity factor for central through-thickness crack in finite plate
K_{sc}	stress intensity factor for surface crack in finite plate
K^W_{ed}	stress intensity factor of welded plate for edge crack
K^W_{cen}	stress intensity factor of welded plate for central through-thickness crack
$K^W_{sc,A}$	stress intensity factor at point A for semi-elliptical surface crack in welded plate
$K^W_{sc,B}$	stress intensity factor at front surface point B for semi-elliptical surface crack in welded plate
$K_{sc,A}$	stress intensity factor at point A for semi-elliptical surface crack in flat plate
$K_{sc,B}$	stress intensity factor at front surface point B for semi-elliptical surface crack in flat plate
$M^A_{k,r}$	stress intensity magnification factor produced by weld profile geometry and residual stress in through-thickness direction
$M^B_{k,r}$	stress intensity magnification factor produced by weld profile geometry and residual stress in through plate width direction
Q	shape factor due to elliptical surface crack
F	stress intensity boundary correction factor

S	remotely applied nominal stress; also fatigue strength of welded butt joint
x	through-thickness distance from weld toe
y	through plate width distance from center of plate
$S_r(x)$	residual stress distribution along x direction
$S_r(y)$	residual stress distribution along y direction
S^*_{rc}	the peak of compressive residual stress on the opposite side of treated surface
$S_w(x)$	local stress distribution along x direction induced by weld geometry
$S_w(y)$	local stress distribution along y direction induced by weld geometry
$S(x)$	resulting stress distribution along potential crack line in x direction ($S(x) = S_r(x) + S_w(x)$)
$S(y)$	resulting stress distribution along potential crack line in y direction ($S(y) = S_r(y) + S_w(y)$)
S_t	residual stress at weld toe surface
S^{max}_{rt}	peak tensile residual stress along x direction
S^{max}_{rc}	peak compressive residual stress along x direction
$m(a,x)$	Bueckner's weight function for edge crack in a finite strip
$G(c,y)$	Kanazawa's weight function for through-thickness central crack in finite plate
R	cyclic stress ratio R ($R = K_{min}/K_{max}$)

Appendix

The equations used for modeling of residual stresses in this study are as follows:

1) In the as-welded condition:

$$S_r(x) = S_r(1-4x/t) \text{ if } 0 \le x \le 0.5t$$

$$S_r(x) = S_r(4x/t-3) \text{ if } 0.5t \le x \le t$$

$$S_r(y) = S_r\cos(2\pi y/t)$$

2) In surface-treated condition:

$$S_r(x) = S_r(x/d_{eff} - 1) \text{ if } 0 \le x \le 1.5d_{eff}$$

$$S_r(x) = S_r[(t' - 0.75d_{eff})\cdot x + 0.5\cdot(t' - 1.5d_{eff})^2]/t'^2 - 1] \text{ if } 1.5d_{eff} \le x \le t$$

where $t' = t - 1.5d_{eff}$

$$S_r(y) = S_r$$

The weight functions used in this study are:

1) Bueckner's weight function (Ref. 16):

$$m(a,x) = [2\pi(a-x)]^{-0.5}\,[1 + m_1(a-x)/a + m_2[(a-x)/a]^2]$$

m_1 and m_2 are functions of the ratio of crack depth to strip width, a/w, and are given as (for $0 \le a/w \le 0.5$):

$$m_1 = A_1 + B_1\,(a/w)^2 + C_1\,(a/w)^6$$

$$m_2 = A_2 + B_2\,(a/w)^2 + C_2(a/w)^6$$

where $A_1 = 0.6147$, $B_1 = 17.1844$, $C_1 = 8.7822$, $A_2 = 0.2502$, $B_2 = 3.2899$, $C_2 = 70.0444$

2) Kanazawa's weight function (Ref. 8):

$$G(c,y) = [2\cdot\sin[\pi(c+y)/w]/w/\sin(2\pi c/w)/\sin(\pi(c-y)/w]]^{0.5}$$

where c = half crack length, w = plate width, and y = distance from plate center line

The local stress distribution induced by weld geometry obtained from FEA and curve fitting are:

$$S_w(x)/S = (1.5521 + 3.6887x + 0.7386x^2)/(1 + 4.867x + 0.4952x^2)$$

$S_w(y)/S = 1.5521$ for $x = 0$, for $t = 6.35$ mm, $\theta = 30$ deg and $r = 1$ mm